

Marina Michalak,
*Mariusz Felczak,
*Bogusław Więcek

Department of Textile Metrology,
Technical University of Łódź,
ul. Żeromskiego 116, 90-924 Łódź, Poland

*Institute of Electronics,
Technical University of Łódź,
ul. Wólczajska 211/215, 90-924 Łódź, Poland
E-mail: marina@p.lodz.pl

Evaluation of the Thermal Parameters of Textile Materials Using the Thermographic Method

Abstract

A continuation of the investigation into a method designed for evaluating thermal properties, especially the thermal conductivity of flat textile products such as nonwovens, is presented in this paper. The method is based on infrared thermography and was described in *Fibres & Textiles in Eastern Europe*, vol. 16, No. 4 (2008) pp. 72-77. In this paper special attention was devoted to nonwovens with and without phase-changing materials (PCM) as well as to the calculation of thermal conductivity. The calculation was based on an optimisation procedure which minimises the temperature difference obtained from modelling and thermovision measurements on both sides of the sample investigated. The main aim of this work was to prove the possibility of investigating flat fibrous materials with temperature dependent thermal parameters. In addition, the authors wanted to confirm the usefulness of the thermographic method for evaluation of the thermal parameters of flat textile materials.

Key words: thermal parameters, thermal conductivity, textile materials, nonwovens, thermovision, heat transmission model.

Introduction

Evaluation of the thermal parameters of new smart textile materials becomes a difficult problem, especially if the materials are made of phase-changing or temperature depended compounds. In the investigations presented in this paper, a method of simultaneous temperature measurement on both sides of the textile sample was used [1 - 7]. This approach is based on using two mirrors with a sample located in between them, as shown in **Figure 1**. The already known methods [8, 9] cannot be applied in such investigations. By measuring the temperature on both sides of fibrous materials, it is possible to evaluate the cross-sectional thermal conductivity of the material, which can, however, differ from the longitudinal.

Heat is delivered to one side of the sample behind the mirrors. The heat flux flows towards the non-heated part of the sample, reaching both sides. The temperature on both sides is slightly different, which is used to estimate the cross-sectional thermal conductivity. Two perpendicular mirrors are placed in front of a thermovision camera. Static and dynamic thermal processes are recorded by the thermo-

vision system and then processed using dedicated software.

In order to verify the experimental resets and correctness of the assumptions, specially prepared teflon samples imitating textile products were used in this work, and next nonwoven samples were tested. It should be emphasised that this work presents preliminary investigations into this method.

Material and structure of the samples investigated

Teflon samples

Preliminary investigations were carried out with a homogenous material. We selected teflon and a samples structure imitating multilayer textile material (**Figure 2**). In the structure of the sample and the procedure of preparation, are more obtained described in [7]. The part measured consists of 3 layers that are located between two mirrors. The longest layer

had thermal contact with a heater. The sample prepared was not isotropic, as it was made from three plates, between which a thin gap of air could be assumed. In order to create the multilayer sample, 3 teflon substrates, each of 3 mm thickness, were firmly connected. To ensure a textile material imitation, holes were made in the middle of the sample, and one external layer was added to get a porosity similar to that existing in real textiles (**Figure 2**). The holes were located in the nodes of a rectangular net, and they had a 1mm diameter with 10 mm spaces [7].

Nonwovens

The investigations were carried out for selected, specially prepared classical and smart nonwovens; the latter containing a phase-changing material in their structure. Stitched nonwovens manufactured at the Technical University of Łódź were used. The microcapsules used, made by Rubitherm, contained material with a phase change at a temperature of 27 °C.

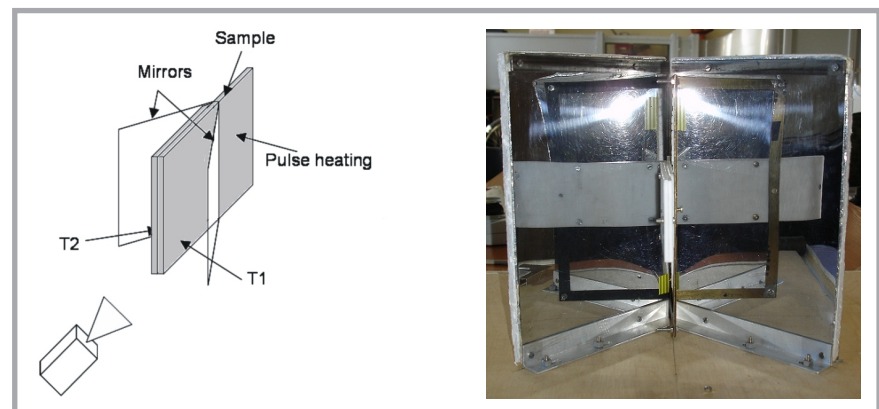


Figure 1. Measuring stand with IR mirrors a) scheme, b) photo of the stand position.

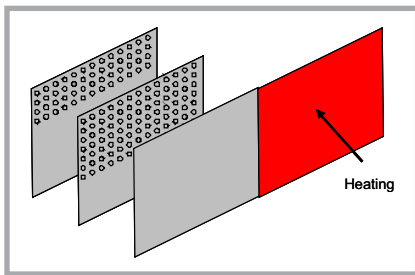


Figure 2. External layer of the experimental teflon sample, connected to a heater; the middle and second external layers are from right to left, with holes imitating the porosity of textile materials.

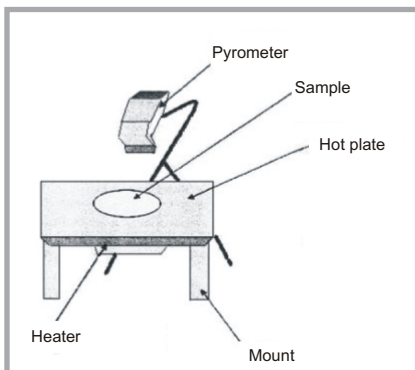


Figure 3. Measuring stand with pyrometer.

They were inserted into the material investigated, consisting of 30% of the total mass of the nonwoven. A description of how the microcapsules were inserted into the textile material is omitted here as it is not relevant in a paper describing a new measurement method. To compare the results, a material without phase change properties, but of similar dimensions, was used. In this paper, we call it 'the reference material', marked 'SO'. Classical nonwovens without phase change active compounds were marked as "0%", and all others according to the content of active material in %.

■ The methods used

The investigations were carried out in parallel using three different measurement systems, i.e. Alambeta apparatus, a specially prepared measuring system with a pyrometer, and a stand within thermovision cameras. All measurements were carried out in an air-conditioned room (but not in a special chamber) with an ambient temperature of 21 ± 1 °C and relative humidity of $65 \pm 5\%$.

An Alambeta meter was described in [9, 10] as well as in our previous works [5, 15, 16]. The apparatus allows to mea-

sure various thermal parameters, such as the thermal resistance, thermal conductivity, thermal absorption and thermal diffusion of homogenous materials.

The measuring stand with a pyrometer is presented in **Figure 3**. The sample was placed on a heated plate. The transient thermal process was recorded until a quasi-stable state was reached at a temperature of 40 °C. The heated plate itself could reach 40 °C after 16 min.

Thermovision measuring stand

During the thermovision measurements (**Figure 1**), the heat flux flows from one side of the sample to the other heating up both sides to different temperature values.

In this investigation the substrates were vertically positioned. The heated zone was outside of the region where the measurements were carried out using an infra-red camera. The special prepared teflon sample, the upper part had holes in two layers in mych in its upper part, whereas the middle part had only a single layer of holes, and the bottom part was without a hole in it.

The heating lasted 50 s. After switching off the electrical power, the heating was still active due to the thermal inertia of the heater. The recording of thermal images was performed at 1 frame/s during 1000 s. An exemplary thermal image excluded from the sequence at $t = 600$ s is presented in **Figure 4**. The IR radiation reflected forms a thermal image which shows the temperature difference on both sides of the material. The higher temperature is on the heated side of the sample. In order to precisely locate the same measuring areas on different images and sequences, a small reference point was used to indicate the proper position. The temperature on both sides of the material was measured during the heating or cooling process.

Characterisation of thermal features

Preliminary thermal results and characteristics

Evaluation of thermal conductivity using an Alambeta meter

Using the Alambeta meter, the heat transfer coefficient λ was measured, and the following results were obtained:

- Classical nonwoven –
 $\lambda = 67.6 \cdot 10^{-3} \text{ W/m} \cdot \text{K}^{-1}$,

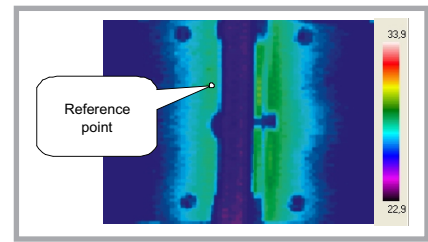


Figure 4. Thermal image taken in the 600th second from switching off the heating.

- PX27 with 30% active material –
 $\lambda = 71.0 \cdot 10^{-3} \text{ W} \cdot \text{m}^{-1} \cdot \text{K}^{-1}$,
- Nonwoven with 30% SO –
 $\lambda = 67.9 \cdot 10^{-3} \text{ W} \cdot \text{m}^{-1} \cdot \text{K}^{-1}$.

The above listed results are difficult to interpret due to the complex thermal state of the PX27 sample.

Pyrometric measurements

Results of the measurement of classical nonwovens (without any active materials) and nonwovens with active (phase changing) compounds obtained by pyrometer measurement are presented in **Figures 5 & 6**. The pyrometer measurements were not very accurate due to difficulties in precise calibration. These measurements were carried out in order to verify the behaviour of PCM material during testing. Characteristics of the temperature versus heating time of nonwovens with and without (classical) PCM compounds are presented in **Figure 5**. **Figure 6** presents the heating up process for nonwovens with a reference material and the classical samples. The temperature difference between the PX27 sample and the nonwoven without active material is visible after 16 min. of the measurement; when the temperature value reaches the level of 27 °C, this becomes the phase-change temperature.

The reference material inserted into the final product had a small impact on the heating up process. The thermal characteristics of products with and without a reference material are practically identical. A temperature value of 40 °C was achievable after 55 min.

It can be seen that the pyrometric measurements showed that nonwovens with and without PCM material have slightly different thermal characteristics.

Thermal characteristics obtained from thermograms

Nonwovens without an active compound, made of PK27 and PK35, with a refer-

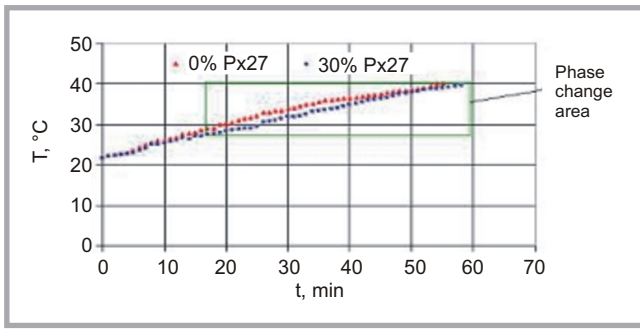


Figure 5. Temperature versus time for nonwoven with 30% PX27 and classical nonwoven (0% of PX 27).

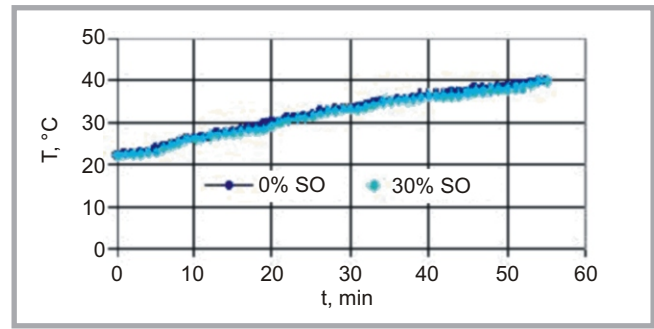


Figure 6. Temperature versus time for reference and classical nonwovens.

ence material were investigated using the stand presented in **Figure 1**, which has 2 mirrors and is equipped with a heater with a Peltier device in order to have the possibility of heating up and cooling down the samples. The heater was powered by 12 W and heat was delivered for 6 min. The initial temperature of the sample was $T_a = 26\text{ }^\circ\text{C}$ (slightly above the ambient temperature of the room, due to the mirrors screening the space). **Figure 7.a** presents an exemple thermal image of classical material without any active phase change additives. **Figure 7.b** shows the time evolution of the temperature for 2 points symmetrically chosen on both sides of the sample presented in **Figure 7.a**.

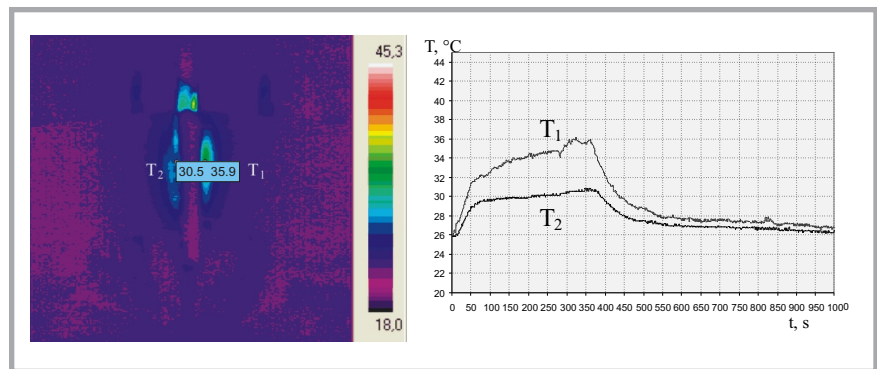


Figure 7. a) Thermal image of a nonwoven without active material after 344 s of the measurement process. b) Temperature versus time for the 2 points shown in Figure 7 for both sides of the sample.

The right side of the sample was heated and the point selected had a temperature of $36\text{ }^\circ\text{C}$, while the corresponding point on the left side reached a temperature of only $30.8\text{ }^\circ\text{C}$. A rise in temperature above the initial temperature was observed in the first 50 s of the heating process. The temperature surplus was $5.5\text{ }^\circ\text{C}$ on the heated side, while at the corresponding point on the opposite side, it was $2.5\text{ }^\circ\text{C}$. In the next period of 300 s of the thermal process, the temperature rose further by only $4\text{ }^\circ\text{C}$ and $2\text{ }^\circ\text{C}$ for heated and unheated sides of the sample, respectively. The difference in temperature between the sides after 360 s of the heating process was $5.5\text{ }^\circ\text{C}$. The material cooled down immediately after the power was switched off. The last frame acquired had a temperature difference of $1\text{ }^\circ\text{C}$ for both sides of the material.

Figure 8 presents a thermal image of PX27 nonwoven after 344 s of the heating process, and in **Figure 8.a** the temperature versus time is shown for this nonwoven.

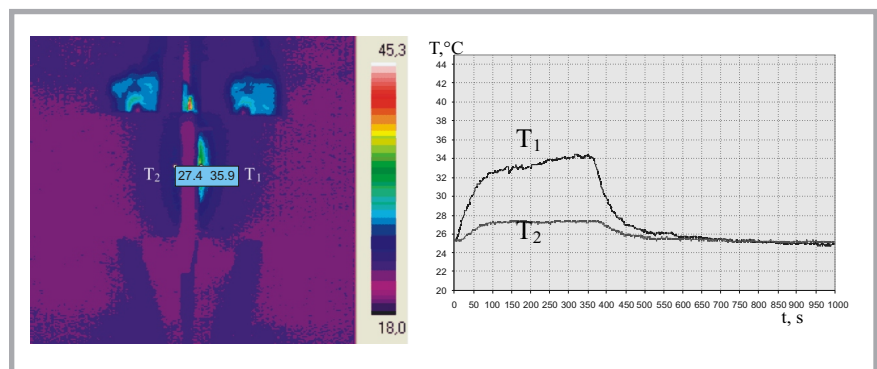


Figure 8. a) Thermal image of a nonwoven made of PX27 after 344s of the measurement process. b) Temperature versus time for a nonwoven made of PX27 for the 2 points shown in Figure 8.

As is visible in **Figure 8.b**, the fastest rise in temperature was observed in the

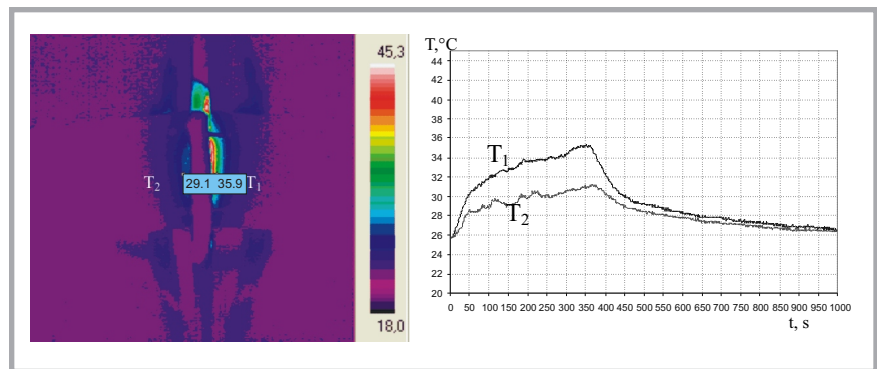


Figure 9. a) Thermal image of a nonwoven made of SO after 344 s of the measurement process. b) Temperature versus time for nonwoven made of SO for the 2 points shown in Figure 9.

first 75 s of heating period for the heated and unheated sides of the sample. The temperature on the warmer and cooler sides of the sample increased by 7 °C and 2 °C, respectively. The temperature of the heated side rose a further 2 °C in the next 300 s, while the unheated side remained at the same temperature until the power was switched off and the cooling down process began. The heated side of the sample warmed up immediately after delivering the power, while the temperature on the unheated side began to rise with a delay of 20 s. The unheated side of the sample reached a temperature of 27 °C, i.e. exactly the level of the phase changing temperature. The cooling down process on the heated side started immediately after the power was switched off - 360 s into the measurement, but on unheated side, cooling began after 380 s. The PX27 nonwoven was characterised by a larger temperature difference (9 °C) between corresponding points on both sides of the sample in comparison with the material without an active compound. The unheated side of the PX27 sample warmed more slowly than the same side on the classical material; a similar effect was observed for the cooling down process as well.

Figure 9.a presents a thermal image of 2 selected points of the reference nonwoven, and **Figure 9.b** shows the time characteristics for these 2 corresponding points, which are symmetrically located on both sides.

The temperature of the selected point on the hot side at the end of the heating-up process was 35 °C, whereas for the corresponding point on the cold side, the temperature reached 31 °C.

As is visible in **Figure 9.a**, the fastest rise in temperature was in the first 60 s of the thermal process. The temperature on the hot and cold sides of the sample increased by 4.5 °C and 2.3 °C, respectively. In the next 300s the temperature of the hot side rose by 9 °C and the cold side by 5 °C. The temperature difference of the selected points on both sides in the last frame of the sequence of thermal images recorded was 4 °C.

The sample made of SO material was characterised by a lower temperature difference between the opposite points on both sides in comparison to the nonwoven with PX27 and the classical material.

From the results presented we can draw a conclusion that the method proposed

allows to investigate the behaviour of PCM material implemented in flat classical fibrous material. For such a material the temperature dependence versus time is almost constant on the unheated side of the substrate, which is due to the phase change compound inserted in the textile material.

Thermal conductivity evaluation by solving a forward and inverse thermal problem by the thermal method

For the determination of thermal parameters, a model was elaborated which was composed of forward and inverse heat transfer parts.

The model

New software was created in order to evaluate the thermal parameters of textile materials using optimisation methods. The new approach is based on the evaluation of the thermal parameters of forward and inverse heat transfer problems. To verify the approach proposed, a teflon sample of rectangular shape, whose width is much smaller than its length, was prepared (**Figure 10**). A pulse of thermal energy was delivered to the material on one side only, and the temperature distribution during heating and cooling was

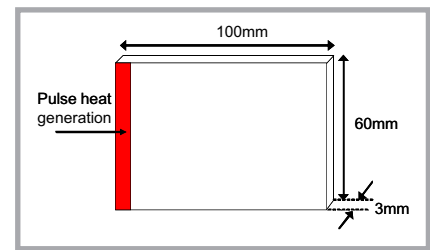


Figure 10. Geometry of the sample with a heat source.

calculated using a 3D thermal model – presented by Equation (1) [12-14]. where:

- x, y, z – coordinates, the distances of heat flow in m,
- $\lambda_x, \lambda_y, \lambda_z$ – thermal conductivity according to x, y, z coordinates in W/(m·K),
- c_p – specific heat in J/kgK,
- ρ – density in kg/m³,
- q – power density in W/m³,
- t – time in s,
- T – temperature in K.

Generally, the thermal conductivity in the textile materials investigated depends on its direction in the material. Conductivity in a cross-sectional direction is, in the majority, higher than in the longitudinal. Because of the complexity of the numerical methods in the research presented, it was assumed that the material is isotropic. In our further investigations the

$$\frac{\partial}{\partial x} \left(\lambda_x \frac{\partial T}{\partial x} \right) + \frac{\partial}{\partial y} \left(\lambda_y \frac{\partial T}{\partial y} \right) + \frac{\partial}{\partial z} \left(\lambda_z \frac{\partial T}{\partial z} \right) + q = c_p \rho \frac{\partial T}{\partial t} \quad (1)$$

Equation 1.

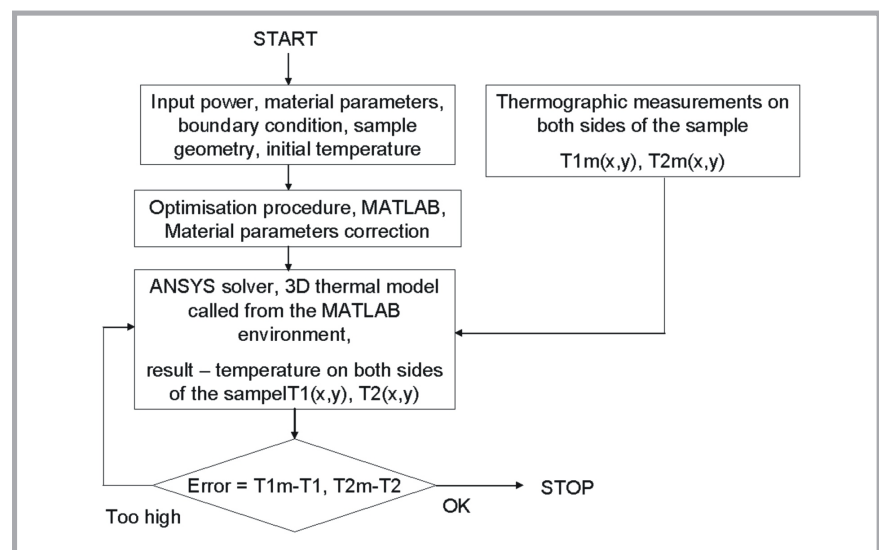


Figure 11. Block diagram of the calculation algorithm.

anisotropy of the materials will be taken into account.

In the forward problem, the temperature distribution, $T = f(q)$, was calculated assuming the values of thermal conductivity (l), specific heat (c_p) and density (r), for a given power density (q) delivered to the sample.

A block diagram calculation of the calculation algorithm is presented in **Figure 11**.

In the inverse problem the temperature distribution on the sample surface is known (e.g. determined by measurements), whereas the thermal parameters of the material, e.g. thermal conductivity λ , are not known. In order to evaluate the values of the unknown thermal parameters, a special new algorithm was developed. For the given power density $q = 133\ 060\ \text{W/m}^3$ and measured temperature distribution $T(x,y)$ on both sides of the sample, the values of λ were evaluated, while r and c_p were assumed as additionally; the boundary conditions for heat dissipation from the sample to the ambient were assumed. The heat transfer coefficient for all surfaces of the sample was set at $8\ \text{W}/(\text{m}^2\text{K})$, which was typical for natural convection, and the ambient temperature was $T_a = 297\ \text{K}$.

In order to solve the inverse problem described, the optimisation procedure was applied using a MATLAB® solver, including the previously mentioned thermal model of a sample implemented in an ANSYS® package (**Figure 11**). The optimisation procedure, written in MATLAB, calls the ANSYS model in an iterative loop. The values of the thermal parameters of the sample are established using the optimisation algorithm. The algorithm stops when the temperature distribution of the sample, obtained from calculations and the experiment, is very close to each other with only a given small error. The accuracy of evaluation of thermal parameters depends on the accuracy of the thermal model, which is solved using the forward thermal algorithm.

Verification of method proposed

In the test simulation of the forward thermal problem, a cuboid sample made of teflon was used. The thermal conduc-

tivity of teflon is known and equal to $\lambda = 0.259\ \text{W}/(\text{m}\cdot\text{K})$. For a given power density q delivered to the material using a heat model based on the Kirchhoff–Fourier law, the temperature $T(x, y, z) = f(q)$ was calculated using the ANSYS® program.

The algorithm implemented chose the starting point for thermal conductivity in the range $\lambda \in (0, 1000)\ \text{W}/(\text{m}\cdot\text{K})$. The temperature obtained by the forward simulation and optimisation procedure was selected for 40 points lying on both sides of the material, i.e., 20 pairs of points.

The temperature $T(x_1, y_1, z_1)$, $T(x_2, y_2, z_2)$, ... $T(x_{20}, y_{20}, z_{20})$ of these points was calculated using the optimisation approach proposed. Subsequently, the temperature difference between the given (forward model) and calculated values of the corresponding points were obtained.

$$\begin{aligned} \Delta T_1 &= T(x_1, y_1, z_1) - T^*(x_1, y_1, z_1), \\ \Delta T_2 &= T(x_2, y_2, z_2) - T^*(x_2, y_2, z_2), \\ &\dots\dots\dots \\ \Delta T_{20} &= T(x_{20}, y_{20}, z_{20}) - T^*(x_{20}, y_{20}, z_{20}), \end{aligned}$$

Then the mean value of temperature difference ΔT_{mean} was determined.

$$\Delta T_{\text{mean}} = \frac{1}{D} \sum_{n=1}^{n=D} \Delta T_i \quad (2)$$

During the following iterations, the algorithm adjusts λ to get ΔT_{mean} as small as possible. The calculus were performed until ΔT_{mean} was equal to zero with a precision of eight digits after the decimal point. **Table 1** shows the results obtained. After the iteration no. 22, changes in the thermal conductivity appear only in the less significant digits.

All the simulations were performed in steady state conditions. The results obtained confirm the possibility of evaluating the thermal conductivity of homogeneous textile materials using the optimisation algorithm based on genetic calculus.

Table 2. Optimisation results for 3-layer material.

Material composition		$\lambda, \text{W}/(\text{m}\cdot\text{K})$
1	plate without holes – Al foil – plate with holes – plate with holes	0.23
2	plate without holes – plate with holes – plate with holes	0.21
3	plate without holes – Al foil – plate with holes – plate without holes	0.28
4	plate without holes – plate with holes – plate without holes	0.26
5	plate without holes – plate without holes – plate without holes	0.30
6	plate without holes – Al foil – plate without holes – plate without holes	0.32

Table 1. Algorithm iterations for teflon.

step	$\lambda, \text{W}/(\text{m}\cdot\text{K})$	$\Delta T_{\text{mean}}, \text{K}$
1	0.38	7.68
2	0.62	7.69
:	:	:
15	0.73	3.74
:	:	:
22	0.26	$3.4 \cdot 10^{-2}$
:	:	:
32	0.26	0.00

Calculations for measured materials

The authors are aware that the experiments performed and results obtained are not for homogenous and isotropic materials, But the approach presented in this paper refers mainly to such materials and, the results in **Table 2** are for anisotropic samples imitating textiles. In this case, the thermal conductivity may only be understood as so-called effective conductivity. As is seen from **Table 2**, it depends on the structure of the material. In these investigations we did not take into account the different values of thermal conductivity dependent on the direction of heat transfer. This will be done in future research.

After proving the correctness of the method proposed, investigations using the measurement results obtained by thermovision were carried out. First, a 3-layer teflon sample imitating a textile material of different porosity, as described above, was attained for the experiment. The temperature distribution on both sides of the sample was registered by the thermovision camera. Three regions of interest were chosen: one with holes in the external and middle layer; the second with a single plate with holes; and the third without any holes (**Figure 2**). For all zones an effective thermal conductivity coefficient was evaluated. The experiments were carried out on the sample presented in **Figure 2**. An aluminum foil was placed at selected areas between the two teflon plates to imitate an electrically conductive textile.

Finally, six different material compositions were obtained:

1. plate without holes – Al foil – plate with holes – plate with holes,
2. plate without holes – plate with holes – plate with holes,
3. plate without holes – Al foil – plate with holes – plate without holes,
4. plate without holes – plate with holes – plate without holes,
5. plate without holes – plate without holes – plate without holes,
6. plate without holes – Al foil – plate without holes – plate without holes.

Additional calculations were made for a sample with 2 plates with holes (plate without – Al foil – plate with holes – plate with holes). The measuring points were located at the holes. A thermal conductivity of $\lambda = 0,23 \text{ W/(m}\cdot\text{K)}$ was obtained. The results of the experiment do not differ very much from the theoretical value of thermal conductivity for teflon. As was expected, the highest value of thermal conductivity was for 3-layers of teflon without holes, while the smallest conductivity was observed in the material with holes and without Al foil. The other configurations of 3-layer material had predicted values of thermal conductivity, i.e., the material with holes filled with air had the lowest value of λ .

■ Conclusions

The method developed is based on simultaneous thermovision measurements of temperature on both sides of the material tested during heating or cooling. Such a process can be used for investigating the thermal characteristics of smart textiles.

The mathematical model developed shows the possibility of evaluating the thermal conductivity of homogenous materials and effective conductivity of fibrous (e.g. nonwovens) materials under stationary conditions.

Investigations on dynamic conditions and anisotropic (classical, as well as smart) materials will be continued.



References

1. Michalak M., Więcek B., Krucińska I., Lis M.: "Thermal Barrier Properties of Nonwovens Multilayer Structures Investigated by Infrared Thermography". VIIth Quantitative Infrared Thermography – QIRT 2004, Brussels, Belgium, 5-8 July, 2004.
2. Michalak M., Więcek B., Krucińska I., Kubsz I.. Modelling and investigation of smart nonwovens with thermostabilization. 1st Aachen-Dresden International Textile Conference, Nov. 28-29, Aachen, 2007, on CD.
3. Michalak M., Więcek B., Krucińska I., Kaczmarek M.. „New Infrared Thermography Method for Investigation of Heat Transport in Nonwovens”. VII International Conference ArchTex-2005, HIGH TECHNOLOGIES IN TEXTILES. Poland, Cracow, September 18 – 20 2005, pp. 13 – 18.
4. Michalak M., Więcek B., Krucińska I., Felczak M. „The Thermal Wave Method for Investigations of Textile Properties.” Vth Quantitative InfraRed Thermography 6 – QIRT'2006.
5. Michalak M., Więcek B., Krucińska I., Felczak M.; The Method of the Wave and Infrared Mirrors for Investigation Thermal Properties of Flat Textile Materials. (in Polish) Proceedings of the 5th Domestic Conference TTP-2006, Ustroń, 16-17 November 2006, pp. 355-360.
6. Michalak M., Więcek B.; Measurements of the Thermal Properties of Flat Textile

Products by a Non-Contact Method., (in Polish). 34th Inter-University Conference of Metrologists, (on CD), Łódź, 24-26 September 2007.

7. Michalak M., Więcek B.. Estimating Thermal Properties of Flat Products by a New Non-contact Method. *Fibres&Textiles in Eastern Europe*, vol.16, Nr 4 (69), 2008, pp. 72-77.
8. Żyliński T.: *Metrologia Włókiennicza*, t.II, wyd.II, WPLiS, Warszawa, 1965.
9. SENSORA Co, *Alambeta Instruction Manual*.
10. Hes L., Dolezal I., *New Method and Equipment for Measuring Thermal Properties of Textiles*, *Journal of Textile Machinery Society of Japan*, Vol. 42, T1-24-T-127, 1989.
11. Maldague Xavier, "Infrared Technology for Nondestructive Testing" ISBN 0-471-18190-0.
12. Welty J., Wicks Ch., Wilson R., Rorrer G., *Fundamentals of Momentum, Heat and Mass Transfer*, John Willey and Son, 2001.
13. Staniszewski B., *Wymiana ciepła*, Ed. Państwowe Wydawnictwo Naukowe, Warszawa 1980.
14. Wiśniewski S., "Wymiana ciepła", ISBN: 83-204-2549-2, Ed. WNT.
15. M. Michalak, B. Więcek, I. Krucińska, M.Lis: "Thermal Barrier Properties of Nonwovens Multilayer Structures Investigated by Infrared Thermography". VIIth Quantitative Infrared Thermography – QIRT 2004, Bruksela, Belgia, 5-8 lipca, 2004.
16. Marina Michalak, Jadwiga Biłska, Izabella Krucińska. „A New Smart Textile Product”, *Proceedings of the 8th International Commodity Science Conference IcomSC'05, CURRENT TRENDS IN COMMODITY SCIENCE*. Poznań, Poland, 28 August – 4 September, 2005, pp. 798 – 806.

■ Received 31.07.2008 Reviewed 19.03.2009



FIBRES & TEXTILES in Eastern Europe

reaches all corners of the world! It pays to advertise your products and services in our magazine! We'll gladly assist you in placing your ads.